Clinical Biomechanics 112 (2024) 106170

Contents lists available at ScienceDirect

Clinical Biomechanics

journal homepage: www.elsevier.com/locate/clinbiomech

Two-to-three times increase in natural hip and lumbar non-sagittal plane kinematics can lead to anterior cruciate ligament injury and cartilage failure scenarios during single-leg landings

Sara Sadeqi [a,*], Grant E. Norte [b], Amanda Murray [c], Deniz U. Erbulut [a], Vijay K. Goel [a]

[a] Engineering Center for Orthopaedic Research Excellence (E-CORE), Departments of Bioengineering and Orthopaedic Surgery, Colleges of Engineering and Medicine, University of Toledo, Toledo, OH 43606, USA
[b] Cognition, Neuroplasticity, & Sarcopenia (CNS) Laboratory, Institute of Exercise Physiology and Rehabilitation Science, University of Central Florida, Orlando, FL 32816, USA
[c] Doctor of Physical Therapy Program, Department of Exercise & Rehabilitation Sciences, College of Health and Human Services, University of Toledo, Toledo, OH 43606, USA

ARTICLE INFO

Keywords:
Knee
ACL injury
Neuromuscular intervention
Finite element analysis
What-if study
Single-leg cross drop

ABSTRACT

Background: Analyzing sports injuries is essential to mitigate risk for injury, but inherently challenging using *in vivo* approaches. Computational modeling is a powerful engineering tool used to access biomechanical information on tissue failure that cannot be obtained otherwise using traditional motion capture techniques.
Methods: We extrapolated high-risk kinematics associated with ACL strain and cartilage load and stress from a previous motion analysis of 14 uninjured participants. Computational simulations were used to induce ACL failure strain and cartilage failure load, stress, and contact pressure in two age- and BMI-matched participants, one of each biological sex, during single-leg cross drop and single-leg drop tasks. The high-risk kinematics were exaggerated in 20% intervals, within their physiological range of motion, to determine if injury occurred in the models. Where injury occurred, we reported the kinematic profiles that led to tissue failure.
Findings: Our findings revealed ACL strains up to 9.99%, consistent with reported failure values in existing literature. Cartilage failure was observed in all eight analyzed conditions when increasing each high-risk kinematic parameter by 2.61 ± 0.67 times the participants' natural landing values. The kinematics associated with tissue failure included peak hip internal rotation of 22.48 ± 19.04°, peak hip abduction of 22.51 ± 9.09°, and peak lumbar rotation away from the stance limb of 11.56 ± 9.78°.
Interpretation: Our results support the ability of previously reported high-risk kinematics in the literature to induce injury and add to the literature by reporting extreme motion limits leading to injurious cases. Therefore, training programs able to modify these motions during single-leg landings may reduce the risk of ACL injury and cartilage trauma.

1. Introduction

Anterior cruciate ligament (ACL) injury is one of the most common traumatic knee injuries among young athletes, and often includes concomitant articular cartilage damage (Tanska et al., 2015). The usage of motion analysis experiments has increased drastically in recent decades as a way to understand the mechanisms of ACL injury by investigating knee biomechanics and patterns of muscle activity during different athletic maneuvers, such as double-leg landings (Taylor et al., 2016), single-leg drop (Nagelli et al., 2020; Taylor et al., 2016), side-step cutting (Maniar et al., 2019), pivoting (Webster et al., 2010), and drop vertical jump (Ueno et al., 2021). Furthermore, researchers have explored the impact of kinetics and kinematics of other body segments or whole-body (WB) on knee biomechanics. Musculoskeletal simulations have been applied to supplement traditional motion analysis experiments by producing information on corresponding muscle forces and their role in ACL loading (Maniar et al., 2019; Ueno et al., 2020). The use of finite element (FE) analyses in combination with the two aforementioned approaches has facilitated access to joint internal stress and contact pressures. Importantly, this combined analytical approach has

* Corresponding author.
E-mail address: sara.sadeqi@utoledo.edu (S. Sadeqi).

https://doi.org/10.1016/j.clinbiomech.2024.106170
Received 18 May 2023; Accepted 4 January 2024
Available online 6 January 2024

allowed researchers to investigate the effects of WB kinematics on knee loads, ligament strains, cartilage stress, contact force, and contact pressure (Sadeqi et al., 2023; Ueno et al., 2021), each of which is essential to better understanding ACL and concomitant injury mechanisms.

A major drawback of these studies is their reliance on motion analysis experiments, which only include data from tasks that are safe for participants in a controlled laboratory environment. These conditions significantly differ from real sports scenarios where actual knee injuries occur. Even video analyses (Krosshaug et al., 2005) of actual injury scenarios report the kinematics that occur after ACL failure, not those leading to injury. Imaging studies investigating bone bruise patterns also have this same limitation (Krosshaug et al., 2005). *In vitro* studies have simulated ACL injury patterns during bipedal landing by applying the external loads of knee abduction moment, internal tibial rotation, anterior shear force, and axial compression to the cadaveric specimen's knee joints using mechanical impact simulators (Bates et al., 2018; Kiapour et al., 2016). While informative, such studies are not able to include muscle activity, account for muscle fatigue, or apply dynamic muscle forces (Hashemi et al., 2007). Computational simulations, on the other hand, have the potential to circumvent these limitations by simulating exaggerated kinetics and kinematics to answer the "what-if" questions (Reinbolt et al., 2011).

Therefore, our primary objective was to extrapolate the kinematic parameters of the whole body (WB) that exhibited the strongest correlations with increased ACL strain, cartilage stress, and contact force, as determined from our previous work (Sadeqi et al., 2023). We aimed to incrementally increase these parameters to replicate tissue damage during two specific landing maneuvers: the single-leg cross drop (SLCD) and the single-leg drop (SLD). The SLCD was chosen due to its inherent multiplanar joint motions, which render it a viable screening tool for injury risk (DiCesare et al., 2015), while the SLD was selected for its widespread utilization among athletes. Failure states were defined as reaching the previously reported thresholds for ACL failure strain (Bates et al., 2017; Bates et al., 2018; Butler et al., 1992; Chandrashekar et al., 2006; Levine et al., 2013; Woo et al., 1991), cartilage failure load (Borrelli Jr et al., 1997), stress (Kerin et al., 1998), or contact pressure (Meyer et al., 2008). We hypothesized that ACL and cartilage failure during single-leg landings could be induced using a validated (Erbulut et al., 2021) knee FE model by manipulating the selected high-risk kinematic parameters in the musculoskeletal models. The outcomes of this objective can confirm whether the high-risk WB kinematics or kinetics reported in the literature can realistically lead to tissue failure at the knee joint. Our secondary objective was to identify the kinematic profiles associated with these high-risk parameters that result in tissue injury. The results of this objective could further our understanding of injury mechanisms and inform how clinicians/athletes train to perform single-leg landings to reduce the risk of ACL and cartilage failure.

2. Methods

In the current study, data from one female and one male participant with matched age and BMI (male:26 yr, height = 172.1 cm, weight = 65.6 kg, BMI = 22.15, and female:26 yr, height = 175.3 cm, weight = 69.1 kg, BMI = 22.51) were used for kinematic manipulations. All participants filled out IRB-approved consent forms. Built upon the results of our preliminary work (Sadeqi et al., 2023) investigating the effect of WB parameters on knee joint biomechanics during single-leg landings, we selected the kinematic parameters which showed the highest correlations with ACL strain, cartilage stress, and contact force in investigations from the motion analysis, musculoskeletal modeling, and FE analyses of fourteen uninjured, physically active participants, during SLCD and SLD to replicate injury scenarios; these variables were operationally defined as "high-risk" kinematic parameters. Detailed correlation data are provided in the supplementary materials.

2.1. In vivo and in silico methods

The *in vivo* and *in silico* methods used have been previously explained (Sadeqi et al., 2023). Briefly, each participant completed the motion analysis experiments by performing SLCD and SLD on both limbs from a 30-cm high platform while wearing 46 reflective markers and repeating three trials for each task. SLCD is when the participant leaves the platform with one limb, but lands on the opposite limb (DiCesare et al., 2015). Marker setup details are presented in Appendix-A. Marker trajectories and force plate data for the dynamic trials were collected and then postprocessed in Visual3D (Version 6.03.6; CMotion). An OpenSim (vers. 4.3, OpenSim) musculoskeletal model with five degrees of freedom at the knee joint (Delp et al., 2007), was used for musculoskeletal simulations. The OpenSim model was scaled for each participant using the data from the static pose to create subject-specific musculoskeletal models. Inverse kinematics, inverse dynamics, and static optimization were used to get the knee kinetics, kinematics, and muscle forces during SLD and SLCD. Inverse kinematics utilizes the body posture derived from marker positions to determine joints' rotations and translations. Inverse dynamics builds upon this data, incorporating ground reaction forces as external loads to solve the equations of motion. This process calculates the joint moments and forces necessary to generate the observed motions. These data were used in a validated finite element model of the knee joint (Erbulut et al., 2021) in Abaqus/Explicit (Abaqus/CAE 2019, Dassault Systemes Simulia Corp., Johnston, RI, USA). Briefly, MR images of a 23-year-old female left knee were utilized in Materialise Mimics (Materialise, Leuven, Belgium) to generate three-dimensional geometries for the knee joint bones and soft tissues. Subsequently, these geometries were smoothed using Geomagic Studio (3D Systems, Rock Hill, SC). Finite element meshes were then incorporated using Hypermesh (Altair, MI), and the model assembly was performed in Abaqus/Explicit. The bone structures were represented as linearly elastic, with distinct coefficients for cancellous and cortical bones. The cruciate and collateral ligaments were modeled using an anisotropic hyper-elastic Holzapfel-Gasser-Ogden model, including viscoelastic behavior (Sadeqi et al., 2021). Articular cartilage properties were integrated using a hyper-elastic Neo-Hookean material model, while the menisci were modeled as transversely isotropic (Erbulut et al., 2021). FE model validation was done in a previous study against *in vitro* data (Bates et al., 2017), replicating bipedal landing from a 30-cm platform (Erbulut et al., 2021). In this work, the FE models were kinetically driven, except for the flexion angle. FE simulations (Ohio Supercomputer Center, n.d.) consisted of two steps. In the first step, the knee was flexed to the amount of flexion at initial foot contact with the ground (IC). IC was defined as when the vertical component of ground reaction force was >10 N (Cowley et al., 2006). The following step simulated the 100 ms after IC, referred to as the landing phase. In this step, external loads of knee abduction moment, internal tibial rotation moment, anterior shear force, and impact force from the landings were applied (Appendix-B).

2.2. Case study

Each landing task was performed on the dominant (SLCD-DL, SLD-DL) and non-dominant (SLCD-NL, SLD-NL) limbs by the two participants chosen for this case study: a total of eight conditions (SLCD-DL-m, SLCD-DL-f, SLD-DL-m, SLD-DL-f, SLCD-NL-m, SLCD-NL-f, SLD-NL-m, and SLD-NL-f).

The kinematic variables analyzed were selected based on the results from our preliminary work that employed correlation, receiver operator characteristic curve, and regression analyses of WB parameters predictive of ACL strain, cartilage stress, and contact forces (Sadeqi et al., 2023). Given the disproportionate emphasis on sagittal plane kinematics in the existing literature, our study intentionally narrows its focus to examine the impact of frontal and transverse plane kinematics. Thus, we did not include sagittal plane kinematics with high correlations. As

greater hip abduction and internal rotation angles on the stance limb, and more lumbar rotation away from the stance limb previously demonstrated the greatest association with tissue damage ($\rho > 0.7$), these were the kinematic parameters we chose to manipulate in the current analysis. Each kinematic variable was systematically exaggerated in 20% increments using OpenSim ver. 4.3 inverse kinematics (IK). Then the new IK was used in the following inverse dynamics and static optimization steps to obtain the modified kinetics and muscle forces, and run the updated FE simulations using a validated knee finite element model (Erbulut et al., 2021). Outputs of the FE analyses were peak values of ACL strain, articular cartilage stress, contact pressure, and contact force during the first 100 ms of landing when ACL strain is reported to be greatest (Kiapour et al., 2014). This process was repeated until ACL failure strain, cartilage failure load, stress, or contact pressure were achieved by the model, then the discrete kinematics values of each variable were recorded at those points.

ACL strain was calculated as the percent change in the ligament length relative to the unloaded state (slack length) (Erbulut et al., 2021; Ueno et al., 2021), and the maximum value was recorded for each condition, *i.e.*, the initial natural landing posture of the participant and the following models with modified kinematics. For peak cartilage stress, contact pressure, and contact force values in each case, the maximum outputs of von Mises stress, CPRESS, and CFORCE contours in Abaqus for the lateral (LTC) and medial (MTC) tibial cartilages were extracted. Changes in the knee moments and quadriceps-to-hamstring ratios of simulated muscle forces from OpenSim resulting from the input of hip and lumbar kinematics manipulations were also recorded for descriptive purposes.

2.3. Statistical analysis

Statistical analysis and data visualization were done using open-source Python libraries ver. 3.8.8 with packages NumPy, Pandas, Matplotlib, and Seaborn. We used Wilcoxon signed-rank tests to determine if the resulting tissue properties statistically differed between the modified (FE-driven) and natural (musculoskeletal-driven) landing conditions. A Benjamini-Hochberg correction was applied to all resulting *P* values to control for a 5% false discovery rate. *P* values ≤ 0.05 were considered statistically significant.

3. Results

A total of 81 simulations were run to produce tissue failures in the eight landing conditions, including female and male SLCD and SLD on the dominant and non-dominant limbs. The new landing postures (*e.g.*, Figs. 1 and 2) created by the input of exaggerated hip and lumbar kinematics (Appendix-C) caused increases in the knee external moments: internal tibial rotation moment increased by 52.53 ± 8.32 Nm ($P = 0.004$), and knee adduction moment increased by 85.27 ± 30.14 Nm ($P = 0.004$). Quadriceps-to-hamstrings ratio also increased by 0.22 ± 0.17 ($P = 0.004$). The increases observed from natural to modified conditions that led to tissue failure were statistically significant; (Appendix-D).

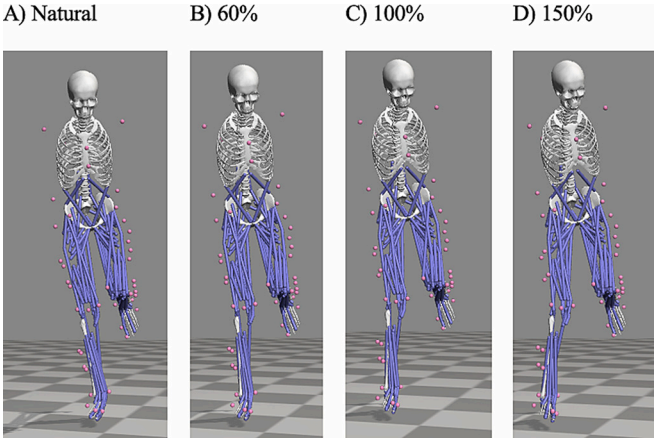

Fig. 2. Changes in the landing posture for the male participant while performing SLCD on the dominant limb. (A) shows the natural landing posture, while B, C, and D show landing postures with exaggerated kinematics by 60%, 100%, and 150% (failure), respectively.

Incremental changes in the output parameters of ACL strain and cartilage biomechanics after each 20% increase in the input hip and lumbar kinematics are presented in Appendix-D. Peak ACL strain (Fig. 3) increased by up to 237%. Peak MTC stress (Fig. 4-A), contact pressure (Fig. 5-A), and contact force (Fig. 6-A) also increased by up to 650%, 297%, and 1643%, respectively. Peak LTC stress (Fig. 4-B) and contact pressure (Fig. 5-B) increased by up to 184% and 154%, respectively. However, peak LTC contact force (Fig. 6-B) decreased in most cases, up to 71% (Table 1). These changes in ACL strain and cartilage biomechanics parameters between the natural landing posture and landing postures leading to tissue failure were statistically significant in all cases (Benjamini-Hochberg corrected Wilcoxon signed-rank tests *P*-values <0.001).

In all cases, cartilage failure criteria (contact force$\geq 4450N$) (Borrelli Jr et al., 1997) were met before extreme increases in peak ACL strain. Maximum values for cartilage contact force, von Mises stress, contact pressure, and ACL strain are presented in Table 2. Typical von Mises stress and contact pressure contours for LTC and MTC are shown in

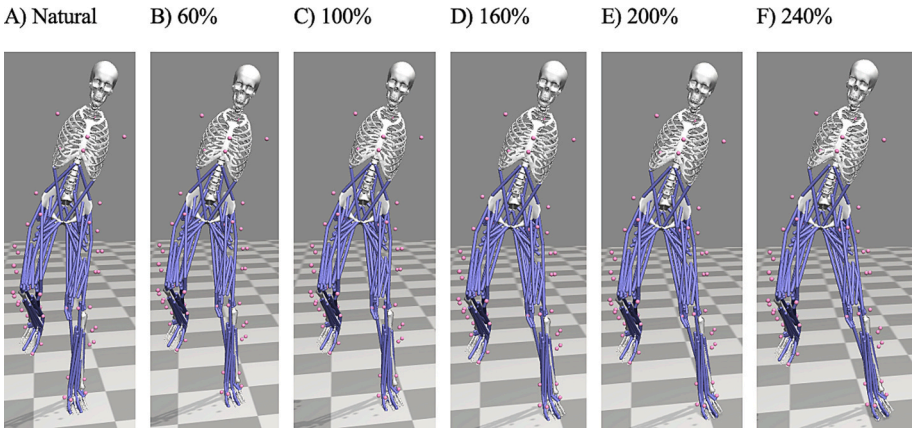

Fig. 1. Changes in the landing posture for the female participant while performing SLD on the non-dominant limb. (A) is the natural landing posture, and B to F show landing postures with exaggerated kinematics by up to 240% (failure).

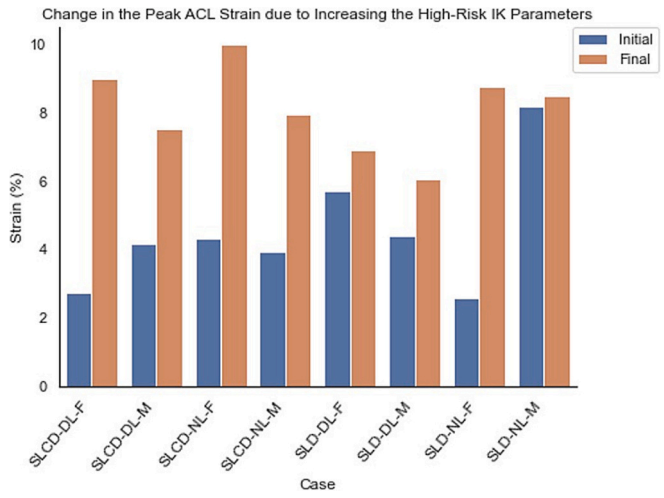

Fig. 3. Maximum changes in peak ACL strain between the participants' natural landing poses (initial) and the modified landing postures leading to failure conditions (final) for male and female SLD and SLCD on the dominant and non-dominant limbs.

Appendix-B.

4. Discussion

To our knowledge, this is the first study to investigate the effect of exaggerating non-sagittal plane high-risk kinematics during single-leg landings on ACL strain, cartilage stress, contact force, and contact pressure by incorporating motion analysis experiments, musculoskeletal simulations, and dynamic FE analyses. Prior investigations of kinematic manipulation are limited by not including an FE component (McLean et al., 2003), which does not allow for evaluation of the soft tissue failure stress within the knee joint. Reliance on 2D musculoskeletal models in the sagittal plane only (Eberle et al., 2019; Heinrich et al., 2020; Heinrich et al., 2022) has also limited our understanding of pathological tissue-specific responses, as they cannot account for the effects of frontal and transverse plane knee moments, which are well demonstrated to increase ACL strain (Kiapour et al., 2016; Sadeqi et al., 2023). In the current work, we used 3D musculoskeletal modeling to account for the non-sagittal plane knee moments and utilized FE simulation to obtain cartilage stress and contact pressure. Our study builds on our previous work (Sadeqi et al., 2023) by evaluating how manipulating the kinematics of proximal body segments to magnitudes unsafe to test *in vivo* affects ACL strain and knee articular cartilage biomechanics during landing tasks that place individuals at risk for injury. Our data indicate that exaggerated hip internal rotation and abduction on the stance limb and lumbar rotation away from the stance limb induced high-risk knee joint biomechanics. Specifically, we observed increases in the knee adduction moment, internal rotation moment, and quadriceps-to-hamstring ratios of the simulated muscle forces to the point that tissue failure occurred at the cartilage and ACL level.

The FE simulations showed great sensitivity with respect to changing the input kinematics. For example, every 20% increase in the input hip and lumbar kinematics led to consistent changes in the output ACL and articular cartilage parameters. Upon increasing the stance hip internal rotation, stance hip abduction, and lumbar rotation away from the stance limb, ACL strain, as well as stress, and contact pressure on both MTC and LTC, and contact force on MTC also increased. MTC contact force exceeded the failure amount of 4450 N (Borrelli Jr et al., 1997) in the extreme increases of the high-risk kinematics in all cases.

Conversely, LTC contact force decreased, which could be because of the extreme changes in the hip kinematics leading to increases in the knee external moments, which affect the tibia position in a way that puts more force on the medial side in each case and reduces the load on the lateral side. This is because the landing is not symmetrical due to the knee abduction/adduction and internal/external rotation of the tibia caused by the external moments. Initial knee alignment related to the coronal tibial slope also affects the tibiofemoral load distribution (Van Rossom et al., 2019). However, external loads have been shown to affect the tibiofemoral load distribution regardless of the tibial slope in the frontal plane (Yang et al., 2010). For example, internal rotation of the tibia and knee adduction, which were seen here, increase the force on the medial side and decrease the force on the lateral component. Although LTC contact force decreased, LTC contact pressure still increased in most cases. That's because the LTC contact area also decreased in each step with the changes in tibia position, and lower contact areas will lead to higher pressures.

The metabolic, biochemical, and biomechanical structure of the articular cartilage causes the knee joint to be one of the most OA-prone

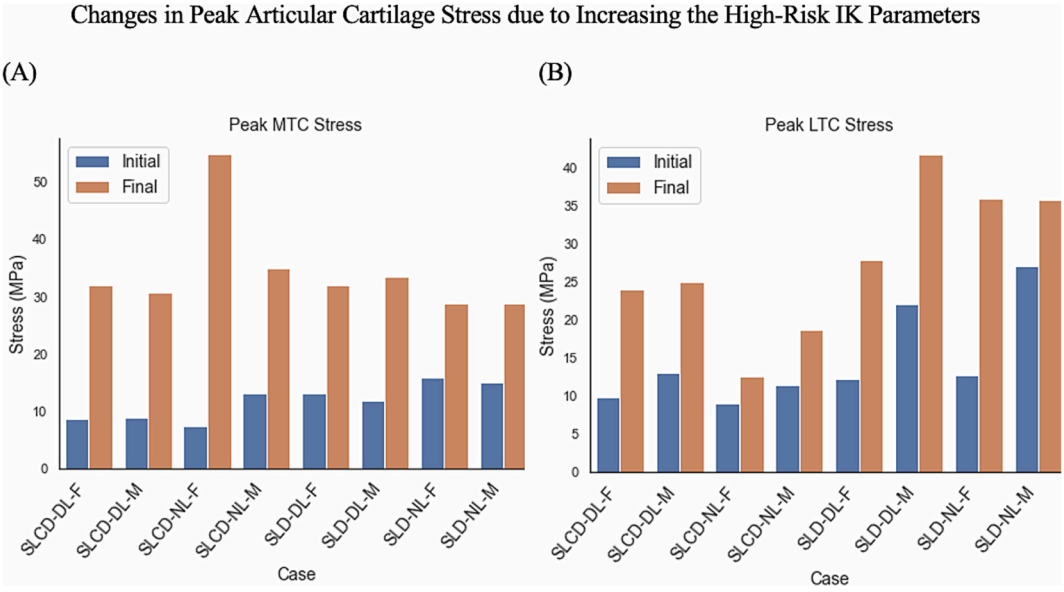

Fig. 4. Maximum changes in (A): peak MTC von Mises stress and (B): peak LTC von Mises stress between the participants' natural landing poses (initial) and the modified landing postures leading to failure conditions (final) for male and female SLD and SLCD on the dominant and non-dominant limbs.

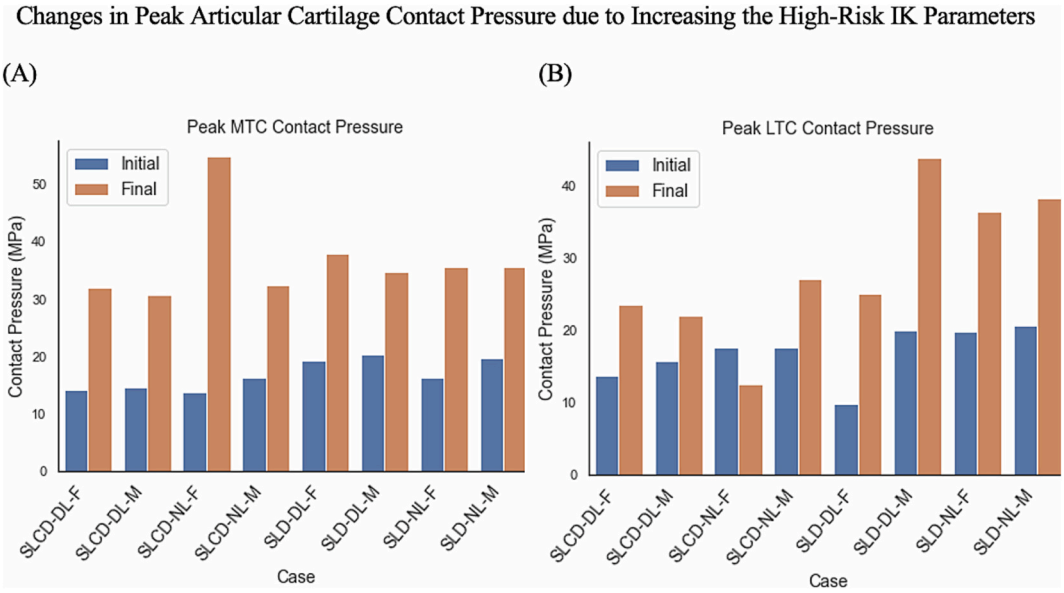

Fig. 5. Maximum changes in (A): peak MTC contact pressure and (B): peak LTC contact pressure between the participants' natural landing poses (initial) and the modified landing postures leading to failure conditions (final) for male and female SLD and SLCD on the dominant and non-dominant limbs.

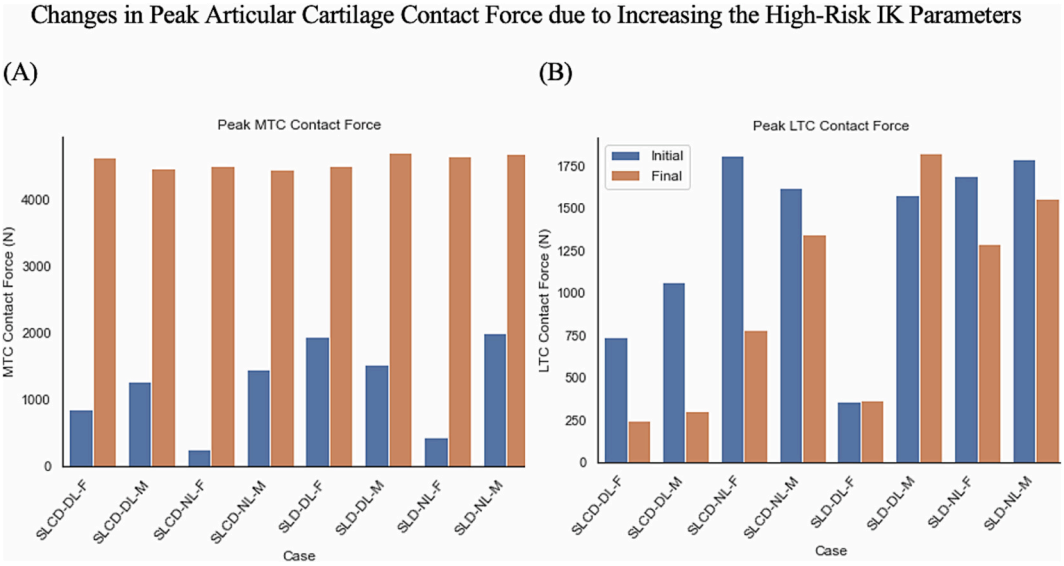

Fig. 6. Maximum changes in (A): peak MTC contact force and (B): peak LTC contact force between the participants' natural landing poses (Initial) and the modified landing postures leading to failure conditions (Final) for male and female SLD and SLCD on the dominant and non-dominant limbs.

human joints (Kuettner and Cole, 2005). One study reported *in vitro* bovine cartilage failure under mean stress values of 35.7 MPa (range: 14–59) (Kerin et al., 1998). *In vitro* experiments simulating impact in rabbit's cartilage reported matrix damage at stresses above 30 MPa and complete cartilage cell death at stresses above 40 MPa. In their *in vivo* setting, superficial matrix damage and cell death happened at 35 MPa stress (Milentijevic et al., 2005). Stresses >25 MPa can initiate chondrocyte death (Buckwalter, 1992; Repo and Finlay, 1977). Pressure film data from cadaveric knees loaded in compression and torsion until ACL failure reported maximum tibiofemoral cartilage pressure of 34 ± 12 MPa and 21 ± 14 MPa, respectively (Meyer et al., 2008). Consistently, in all the cases with failure cartilage load, failure cartilage stress and contact pressures were also seen in our simulations (Table 2).

Failure strain for ACL in the literature varies widely depending on the loading conditions, with reported values ranging from 6.6% to 35% (Bates et al., 2017; Bates et al., 2018; Butler et al., 1992; Chandrashekar et al., 2006; Levine et al., 2013) (28 ± 7% (Chandrashekar et al., 2006), 18.7 ± 10% (Levine et al., 2013), 15.3 ± 8.7% (Bates et al., 2018), and 18.8 ± 6.2% (Bates et al., 2017)). In this study, the peak ACL strains at the time of cartilage failure ranged from 6.06 to 9.99%. In the OpenSim model, muscle forces increased in response to the increased kinematics, which could have protected ACL from very large strains. However, since quadriceps-to-hamstrings muscle force ratios also increased in all cases, increases in ACL strain were observed, although not to the extent of ACL failure. It should also be noted that in athletic conditions, muscles may not perform optimally, and these reported strains under combined loading in combination with high compressive loads might still lead to ACL rupture. Additionally, based on an *in vitro* study of the tensile properties of 10 male and 10 female ACLs, female ACLs failed at a lower strain (8.3% lower strain at failure) relative to their male counterparts (Chandrashekar et al., 2006). Therefore, these extreme hip and lumbar kinematics changes might lead to injury more often in females. Higher

Table 1
Percent changes in peak ACL strain, peak articular cartilage contact force, contact pressure, and von Mises stress between the participants' natural landing pose and final postures leading to tissue failure during female and male SLCD and SLD on the dominant and non-dominant limbs.

Case	Δ peak ACL strain (%)	Δ peak MTC contact Force (%)	Δ peak LTC contact Force (%)	Δ peak MTC contact Pressure (%)	Δ peak LTC contact Pressure (%)	Δ peak MTC Stress (%)	Δ peak LTC Stress (%)
SLCD-DL-f	227.97	438.10	−66.52	126.09	71.58	269.70	145.15
SLCD-DL-m	80.91	253.23	−71.23	108.93	40.43	249.87	92.17
SLCD-NL-f	131.52	1643.08	−57.00	297.29	−29.18	650.31	38.67
SLCD-NL-m	102.23	205.53	−16.65	97.23	54.07	168.79	62.72
SLD-DL-f	21.47	132.38	2.64	97.00	153.80	141.72	128.84
SLD-DL-m	37.23	208.49	15.81	70.72	120.02	183.51	89.12
SLD-NL-f	237.45	982.84	−23.73	119.04	83.81	82.03	183.89
SLD-NL-m	4.00	135.23	−12.98	79.83	85.56	91.76	32.24

Table 2
Peak values of ACL strain, articular cartilage contact force, contact pressure, and von Mises stress during the exaggerated landing postures leading to tissue failure for female and male SLCD and SLD on the dominant and non-dominant limbs.

Case	Peak ACL strain (%)	Peak MTC contact Force (N)	Peak LTC contact Force (N)	Peak MTC contact Pressure (MPa)	Peak LTC contact Pressure (MPa)	Peak MTC Stress (MPa)	Peak LTC Stress (MPa)
SLCD-DL-f	9.01	4631.04	246.91	31.97	23.51	32.04	23.95
SLCD-DL-m	7.54	4474.56	306.18	30.63	22.04	30.81	24.89
SLCD-NL-f	9.99	4519.65	780.07	54.93	12.52	54.93	12.52
SLCD-NL-m	7.95	4449.70	1348.27	32.32	27.15	34.98	18.67
SLD-DL-f	6.92	4514.13	369.63	37.97	24.98	31.92	27.89
SLD-DL-m	6.06	4709.55	1824.45	34.85	43.90	33.41	41.67
SLD-NL-f	8.75	4651.27	1292.46	35.56	36.36	28.73	35.79
SLD-NL-m	8.50	4699.40	1560.36	35.50	38.26	28.72	35.64

increases in ACL strain in the female participant (Table 1) are also consistent with the reported findings that injury risk reduction programs were more effective in females (Webster and Hewett, 2018).

Literature has been uncertain regarding the effect of trunk axial rotation, hip internal/external rotation, and hip ab/adduction on the knee biomechanics during dynamic activities. Both hip internal (Finnoff et al., 2011) and external (Ishida et al., 2021) rotations affect knee loading, and large amounts of these rotations have been associated with increased knee kinematics, such as knee abduction or internal tibial rotation angles, that increase the risk of ACL injury. Both hip internal/external (Malloy et al., 2016) rotator strength and hip adductors/abductors strength (Almeida et al., 2022; Ferreira et al., 2015) were shown to protect the knee against high-risk kinematics and kinetics. Lumbopelvic-hip stability protects the knee by reducing knee valgus angles and increasing the hamstring-to-quadriceps coactivation (Jeong et al., 2021). Torso axial rotation in the opposite direction of the cut during sidestep cutting was shown to put the athletes at a higher risk of injuries (Dempsey et al., 2007). Video analyses also reported that trunk axial rotation away from the injured leg was seen more frequently than trunk axial rotation towards the injured leg during ACL injuries (Song et al., 2021). We applied the same three factors to all tasks (SLCD and SLD on the dominant and non-dominant limbs) to see if overall recommendations could be made for different variations of single-leg landings. These motion manipulations led to increases in the cartilage force, pressure, stress, and ACL strain in all cases.

4.1. Limitations

Our findings must be interpreted in the context of existing limitations. Firstly, data only from two participants (one male and one female) were used for kinematics manipulation. Also, the participants were physically active but not athletes. Thus, their unfamiliarity with the tasks could have affected their postures. Therefore, further investigation by utilizing more participants from the athletic population is required to determine the limits of motion with regard to ACL failure or cartilage damage, which can be recommended to the majority of athletes. Additionally, we used the same magnitudes of GRF for each landing in the modified postures as the initial pose since only experimental GRF data from each natural posture was available (8 cases). However, the landing posture affects the ground reaction forces, and simulating foot-ground contact models in OpenSim could help in determining the modified GRFs (Saraiva et al., 2022). Applying the same GRF for each exaggeration step of the same tasks would reflect the sole effect of changing the hip and lumbar kinematics on the knee biomechanics. Moreover, the same finite element model was used for both participants. Future work may use the medical images of the same participants performing the tasks to create the FE models to capture the effects of their unique joint geometries. Lastly, muscle fatigue was not accounted for. Most sports injuries happen when the muscles are fatigued (Lin et al., 2022) and cannot provide their protective role (Maniar et al., 2022). So, kinematic increases lower than the ones reported here might still lead to injury in actual sports events. Future work may benefit from using EMG-driven analyses (Hume et al., 2019) and applying muscle fatigue and recovery models (Giat et al., 1996) to their investigations. Another aspect is

that the combined effect of three factors was tested here, making it difficult to attribute the increases in cartilage biomechanics parameters and ACL strain to a single factor. Future work may look at the effect of individual factors; however, body segment kinematics are related to each other in real cases, and injuries mostly happen under combined and multiplanar loadings (Kiapour et al., 2016).

Based on the outcomes of our analyses, we recommend that increased hip internal rotation, hip abduction, and lumbar rotation away from the stance limb should be avoided during single-leg landings to prevent the medial knee component from undergoing excessive loads and reduce ACL strain.

5. Conclusions

This study successfully produced ACL failure and knee cartilage damage in computational models by increasing hip internal rotation angles, hip abduction angles, and lumbar rotation away from the stance limb during single-leg landings to simulate the high-risk kinematics that are not safe to be tested *in vivo*. Our work confirmed that the high-risk kinematics reported in the literature could lead to injury when increased to the limits reported here. These results can be used in developing injury risk reduction programs for athletes. These types of studies should be expanded by including the effect of other high-risk kinematics during various athletic maneuvers to access more details on injury mechanisms and prevention without imposing any risks on the participants.

Author contributions statement

All authors have made substantial contributions to (1) the conception and design of the study, acquisition of data, and analysis and interpretation of data, (2) drafting the article and revising it critically for important intellectual content, and (3) final approval of the version to be submitted.

Declaration of competing interest

None.

Appendix A. Supplementary data

Supplementary data to this article can be found online at https://doi.org/10.1016/j.clinbiomech.2024.106170.

References

Almeida, G.P.L., Monteiro, I.O., Tavares, M.L.A., Porto, P.L.S., Albano, T.R., Marques, A. P., 2022. Hip abductor versus adductor strengthening for clinical outcomes in knee symptomatic osteoarthritis: a randomized controlled trial. Musculoskelet Sci. Pract. 102575. https://doi.org/10.1016/j.msksp.2022.102575.

Bates, N.A., Schilaty, N.D., Nagelli, C.V., Krych, A.J., Hewett, T.E., 2017. Novel mechanical impact simulator designed to generate clinically relevant anterior cruciate ligament ruptures. Clin. Biomech. 44, 36–44. https://doi.org/10.1016/j.clinbiomech.2017.03.005.

Bates, N.A., Schilaty, N.D., Nagelli, C.V., Krych, A.J., Hewett, T.E., 2018. Validation of noncontact anterior cruciate ligament tears produced by a mechanical impact simulator against the clinical presentation of injury. Am. J. Sports Med. 46 (9), 2113–2121. https://doi.org/10.1177/0363546518776621.

Borrelli Jr., J., Torzilli, P.A., Grigiene, R., Helfet, D.L., 1997. Effect of impact load on articular cartilage: development of an intra-articular fracture model. J. Orthop. Trauma 11 (5), 319–326. https://doi.org/10.1097/00005131-199707000-00003.

Buckwalter, J.A., 1992. Mechanical injuries of articular cartilage. Iowa Orthop. J. 12, 50.

Butler, D.L., Guan, Y., Kay, M.D., Cummings, J.F., Feder, S.M., Levy, M.S., 1992. Location-dependent variations in the material properties of the anterior cruciate ligament. J. Biomech. 25 (5), 511–518. https://doi.org/10.1016/0021-9290(92)90091-E.

Chandrashekar, N., Mansouri, H., Slauterbeck, J., Hashemi, J., 2006. Sex-based differences in the tensile properties of the human anterior cruciate ligament. J. Biomech. 39 (16), 2943–2950. https://doi.org/10.1016/j.jbiomech.2005.10.031.

Cowley, H.R., Ford, K.R., Myer, G.D., Kernozek, T.W., Hewett, T.E., 2006. Differences in neuromuscular strategies between landing and cutting tasks in female basketball and soccer athletes. J. Athl. Train. 41 (1), 67.

Delp, S.L., et al., Nov 2007. OpenSim: open-source software to create and analyze dynamic simulations of movement. IEEE Trans. Biomed. Eng. 54 (11), 1940–1950. https://doi.org/10.1109/TBME.2007.901024.

Dempsey, A.R., Lloyd, D.G., Elliott, B.C., Steele, J.R., Munro, B.J., Russo, K.A., 2007. The effect of technique change on knee loads during sidestep cutting. Med. Sci. Sports Exerc. 39 (10), 1765–1773. https://doi.org/10.1249/mss.0b013e31812f56d1.

DiCesare, C.A., et al., 2015. Reliability of 3-dimensional measures of single-leg cross drop landing across 3 different institutions: implications for multicenter biomechanical and epidemiological research on ACL injury prevention. Orthop. J. Sports Med. 3 (12) https://doi.org/10.1177/2325967115617905, 2325967115617905.

Eberle, R., Heinrich, D., van den Bogert, A., Oberguggenberger, M., Nachbauer, W., 2019. An approach to generate noncontact ACL-injury prone situations on a computer using kinematic data of non-injury situations and Monte Carlo simulation. Comput. Methods Biomech. Biomed. Engin. 22 (1), 3–10. https://doi.org/10.1080/10255842.2018.1522534.

Erbulut, D.U., Sadeqi, S., Summers, R., Goel, V.K., Oct 1 2021. Tibiofemoral cartilage contact pressures in athletes during landing: a dynamic finite element study. J. Biomech. Eng. 143 (10), 101006 https://doi.org/10.1115/1.4051231.

Ferreira, G.E., Robinson, C.C., Wiebusch, M., de Mello Viero, C.C., da Rosa, L.H.T., Silva, M.F., 2015. The effect of exercise therapy on knee adduction moment in individuals with knee osteoarthritis: a systematic review. Clin. Biomech. 30 (6), 521–527. https://doi.org/10.1016/j.clinbiomech.2015.03.028.

Finnoff, J.T., Hall, M.M., Kyle, K., Krause, D.A., Lai, J., Smith, J., 2011. Hip strength and knee pain in high school runners: a prospective study. PM&R 3 (9), 792–801. https://doi.org/10.1016/j.pmrj.2011.04.007.

Giat, Y., Mizrahi, J., Levy, M., 1996. A Model of Fatigue and Recovery in paraplegic's Quadriceps Muscle Subjected to Intermittent FES. https://doi.org/10.1115/1.2796018.

Hashemi, J., Chandrashekar, N., Jang, T., Karpat, F., Oseto, M., Ekwaro-Osire, S., 2007. An alternative mechanism of non-contact anterior cruciate ligament injury during jump-landing: in-vitro simulation. Exp. Mech. 47 (3), 347–354. https://doi.org/10.1007/s11340-007-9043-y.

Heinrich, D., van den Bogert, A.J., Csapo, R., Nachbauer, W., 2020. A model-based approach to predict neuromuscular control patterns that minimize ACL forces during jump landing. Comput. Methods Biomech. Biomed. Engin. 24 (6), 612–622. https://doi.org/10.1080/10255842.2020.1842376.

Heinrich, D., van den Bogert, A.J., Nachbauer, W., 2022. Predicting neuromuscular control patterns that minimize ACL forces during injury-prone jump-landing manoeuvres in downhill skiing using a musculoskeletal simulation model. Eur. J. Sport Sci. 1–11. https://doi.org/10.1080/17461391.2022.2064770.

Hume, D.R., Navacchia, A., Rullkoetter, P.J., Shelburne, K.B., 2019. A lower extremity model for muscle-driven simulation of activity using explicit finite element modeling. J. Biomech. 84, 153–160. https://doi.org/10.1016/j.jbiomech.2018.12.040.

Ishida, T., et al., 2021. Larger hip external rotation motion is associated with larger knee abduction and internal rotation motions during a drop vertical jump. Sports Biomech. 1–15. https://doi.org/10.1080/14763141.2021.1881151.

Jeong, J., Choi, D.-H., Shin, C.S., 2021. Core strength training can alter neuromuscular and biomechanical risk factors for anterior cruciate ligament injury. Am. J. Sports Med. 49 (1), 183–192. https://doi.org/10.1177/0363546520972990.

Kerin, A., Wisnom, M., Adams, M., 1998. The compressive strength of articular cartilage. Proc. Inst. Mech. Eng. H 212 (4), 273–280. https://doi.org/10.1243/0954411981534051.

Kiapour, A.M., Quatman, C.E., Goel, V.K., Wordeman, S.C., Hewett, T.E., Demetropoulos, C.K., 2014. Timing sequence of multi-planar knee kinematics revealed by physiologic cadaveric simulation of landing: implications for ACL injury mechanism. Clin. Biomech. 29 (1), 75–82. https://doi.org/10.1016/j.clinbiomech.2013.10.017.

Kiapour, A.M., et al., 2016. Strain response of the anterior cruciate ligament to uniplanar and multiplanar loads during simulated landings: implications for injury mechanism. Am. J. Sports Med. 44 (8), 2087–2096. https://doi.org/10.1177/0363546516640499.

Krosshaug, T., Andersen, T.E., Olsen, O.O., Myklebust, G., Bahr, R., 2005. Research approaches to describe the mechanisms of injuries in sport: limitations and possibilities. Br. J. Sports Med. 39 (6), 330–339. https://doi.org/10.1136/bjsm.2005.018358.

Kuettner, K., Cole, A., 2005. Cartilage degeneration in different human joints. Osteoarthr. Cartil. 13 (2), 93–103. https://doi.org/10.1016/j.joca.2004.11.006.

Levine, J.W., et al., Feb 2013. "clinically relevant injury patterns after an anterior cruciate ligament injury provide insight into injury mechanisms," (in English). Am. J. Sports Med. 41 (2), 385–395. https://doi.org/10.1177/0363546512465167.

Lin, H.-T., Kuo, W.-C., Chen, Y., Lo, T.-Y., Li, Y.-I., Chang, J.-H., 2022. Effects of fatigue in lower Back muscles on basketball jump shots and landings. Phys. Act. Health 6 (1).

Malloy, P., Morgan, A., Meinerz, C., Geiser, C.F., Kipp, K., 2016. Hip external rotator strength is associated with better dynamic control of the lower extremity during landing tasks. J. Strength Cond. Res. 30 (1), 282. https://doi.org/10.1519/JSC.0000000000001069.

Maniar, N., Schache, A.G., Cole, M.H., Opar, D.A., 2019. Lower-limb muscle function during sidestep cutting. J. Biomech. 82, 186–192. https://doi.org/10.1016/j.jbiomech.2018.10.021.

Maniar, N., Cole, M.H., Bryant, A.L., Opar, D.A., 2022. Muscle force contributions to anterior cruciate ligament loading. Sports Med. 1–14. https://doi.org/10.1007/s40279-022-01674-3.

McLean, S.G., Su, A., van den Bogert, A.J., 2003. Development and validation of a 3-D model to predict knee joint loading during dynamic movement. J. Biomech. Eng. 125 (6), 864–874. https://doi.org/10.1115/1.1634282.

Meyer, E.G., Baumer, T.G., Slade, J.M., Smith, W.E., Haut, R.C., 2008. Tibiofemoral contact pressures and osteochondral microtrauma during anterior cruciate ligament rupture due to excessive compressive loading and internal torque of the human knee. Am. J. Sports Med. 36 (10), 1966–1977. https://doi.org/10.1177/0363546508318046.

Milentijevic, D., Rubel, I.F., Liew, A.S., Helfet, D.L., Torzilli, P.A., 2005. An in vivo rabbit model for cartilage trauma: a preliminary study of the influence of impact stress magnitude on chondrocyte death and matrix damage. J. Orthop. Trauma 19 (7), 466–473. https://doi.org/10.1097/01.bot.0000162768.83772.18.

Nagelli, C., et al., 2020. Neuromuscular training improves self-reported function and single-leg landing hip biomechanics in athletes after anterior cruciate ligament reconstruction. Orthop. J. Sports Med. 8 (10), 2325967120959347.

Ohio Supercomputer Center. http://osc.edu/ark:/19495/f5s1ph73 (accessed).

Reinbolt, J.A., Seth, A., Delp, S.L., 2011. Simulation of human movement: applications using OpenSim. Procedia Iutam 2, 186–198. https://doi.org/10.1016/j.piutam.2011.04.019.

Repo, R., Finlay, J., 1977. Survival of articular cartilage after controlled impact. J. Bone Joint Surg. Am. 59 (8), 1068–1076.

Sadeqi, S., Summers, R., Erbulut, D.U., Goel, V.K., 2021. Optimization of material coefficients in the Holzapfel-gasser-Ogden material model for the Main four ligaments of the knee joint-a finite element study. Appl. Math. 12 (12), 1166–1188. https://doi.org/10.4236/am.2021.1212075.

Sadeqi, S., Norte, G.E., Murray, A., Erbulut, D.U., Goel, V.K., 2023. Effect of whole body parameters on knee joint biomechanics: implications for ACL injury prevention during single-leg landings. Am. J. Sports Med. 51 (8), 2098–2109. https://doi.org/10.1177/03635465231174899.

Saraiva, L., da Silva, M.R., Marques, F., da Silva, M.T., Flores, P., 2022. A review on foot-ground contact modeling strategies for human motion analysis. Mech. Mach. Theory 177, 105046. https://doi.org/10.1016/j.mechmachtheory.2022.105046.

Song, Y., Li, L., Hughes, G., Dai, B., 2021. Trunk motion and anterior cruciate ligament injuries: a narrative review of injury videos and controlled jump-landing and cutting tasks. Sports Biomech. 1–19. https://doi.org/10.1080/14763141.2021.1877337.

Tanska, P., Mononen, M.E., Korhonen, R.K., 2015. A multi-scale finite element model for investigation of chondrocyte mechanics in normal and medial meniscectomy human knee joint during walking. J. Biomech. 48 (8), 1397–1406. https://doi.org/10.1016/j.jbiomech.2015.02.043.

Taylor, J.B., Ford, K.R., Nguyen, A.-D., Shultz, S.J., 2016. Biomechanical comparison of single-and double-leg jump landings in the sagittal and frontal plane. Orthop. J. Sports Med. 4 (6) https://doi.org/10.1177/2325967116655158, 2325967116655158.

Ueno, R., et al., Apr 16 2020. "knee abduction moment is predicted by lower gluteus medius force and larger vertical and lateral ground reaction forces during drop vertical jump in female athletes," (in English). J. Biomech. 103, 109669 https://doi.org/10.1016/j.jbiomech.2020.109669.

Ueno, R., Navacchia, A., Schilaty, N.D., Myer, G.D., Hewett, T.E., Bates, N.A., Mar 2021. Anterior cruciate ligament loading increases with pivot-shift mechanism during asymmetrical drop vertical jump in female athletes. Orthop. J. Sports Med. 9 (3) https://doi.org/10.1177/2325967121989095, 2325967121989095.

Van Rossom, S., Wesseling, M., Smith, C.R., Thelen, D.G., Vanwanseele, B., Jonkers, I., 2019. The influence of knee joint geometry and alignment on the tibiofemoral load distribution: a computational study. Knee 26 (4), 813–823.

Webster, K.E., Hewett, T.E., Oct 2018. Meta-analysis of meta-analyses of anterior cruciate ligament injury reduction training programs. J. Orthop. Res. 36 (10), 2696–2708. https://doi.org/10.1002/jor.24043.

Webster, K.E., McClelland, J.A., Wittwer, J.E., Tecklenburg, K., Feller, J.A., 2010. Three dimensional motion analysis of within and between day repeatability of tibial rotation during pivoting. Knee 17 (5), 329–333.

Woo, S.L.-Y., Hollis, J.M., Adams, D.J., Lyon, R.M., Takai, S., 1991. Tensile properties of the human femur-anterior cruciate ligament-tibia complex: the effects of specimen age and orientation. Am. J. Sports Med. 19 (3), 217–225.

Yang, N.H., Canavan, P.K., Nayeb-Hashemi, H., 2010. The effect of the frontal plane tibiofemoral angle and varus knee moment on the contact stress and strain at the knee cartilage. J. Appl. Biomech. 26 (4), 432–443. https://doi.org/10.1123/jab.26.4.432.